Talanta 88 (2012) 450–455

Contents lists available at SciVerse ScienceDirect

Talanta

journal homepage: www.elsevier.com/locate/talanta

DNA G-quadruplex-templated formation of the fluorescent silver nanocluster and its application to bioimaging

Jun Ai[a,b], Weiwei Guo[a,b], Bingling Li[a,b], Tao Li[a,b], Dan Li[a,b], Erkang Wang[a,*]

[a] State Key Laboratory of Electroanalytical Chemistry, Changchun Institute of Applied Chemistry, Chinese Academy of Sciences, Changchun, Jilin 130022, People's Republic of China
[b] Graduate School of the Chinese Academy of Sciences, Beijing 100039, People's Republic of China

ARTICLE INFO

Article history:
Received 28 June 2011
Received in revised form 21 October 2011
Accepted 26 October 2011
Available online 9 November 2011

Keywords:
G-quadruplex
Silver nanocluster
Nucleolin
Bioimaging

ABSTRACT

Herein, a novel kind of silver nanocluster is synthesized simply by mixing G-quadruplex template with silver ions and reduction reagent ($NaBH_4$, here). AS1411 (a G-quadruplex that can bind nucleolin over-expressed in cancer cells) is used as the main model template to prove the synthesis protocol and its potential application. We used fluorescence assay, CD, MALDI TOF MS, and TEM to characterize the silver nanocluster. It is found that after formation of the silver nanocluster, AS1411 still keeps its structure and is able to bind with nucleolin in cancer cell. Meanwhile, this binding behavior can greatly enhance the fluorescence intensity of the silver nanocluster. This property can be directly employed into bioimaging HeLa cells. The cell toxicity (3-[4,5-dimethylthiazolyl-2]-2,5-diphenyltetrazolium bromide, MTT) assay demonstrated that the silver nanocluster has only little affect on the cytotoxicity to the cells, which further proves the applicability of the method in tumor cell imaging. At last, the universality of the synthesis protocol is verified by using a series of other G-quadruplex sequences as templates. For a lot of functional nucleic acids, such as human telomeres and certain aptamers, are with G-rich sequences and can fold into G-quadruplexes in functioning conditions, our method displays a promising application space in future researches.

1. Introduction

Noble metal nanoclusters, consisting of a few metal atoms, have gained great attention due to their unique fluorescence properties and potential applications in the field of biological imaging. In particular, silver nanoclusters synthesized using polycytosines as matrices have attracted more attention in the field of medicine, pharmacology and biology. Silver nanoclusters encapsulated by the single-stranded oligonucleotide dC12 arguably consist of the most promising system for their very high photoemission rates and their excellent photostability [1–4]. It is generally known that silver ion and C base are easily incorporated. The high affinity of Ag^+ for deoxyribonucleic acid (DNA) bases has enabled creation of short oligonucleotide-encapsulated silver nanoclusters without formation of large nanoparticles. Time-dependent formation of nanocluster sizes ranging from Ag_1 to Ag_4 oligonucleotide was observed with strong characteristic electronic transitions between 400 and 600 nm [5]. The reduction of silver cations bound to the oligonucleotide dC12 was used to form silver nanoclusters. Mass spectra show that the oligonucleotides have 2–7 silver atoms that form multiple species, as evidenced from the number of transitions in the fluorescence and absorption spectra [6,7]. These silver nanoclusters made of few-atom offer great potential in pushing in vitro, and possibly in vivo, single-molecule study faster and also in longer time scales [1–4]. DNA-encapsulated silver nanoclusters are readily conjugated to proteins and serve as alternatives to organic dyes and semiconductor quantum dots. DNA/silver nanoclusters of guanine-rich DNA ("guanine" is abbreviated to "G") sequences could emit red fluorescence and enhanced 500-fold when placed in proximity to cytosine-rich DNA ("cytosine" is abbreviated to "C") [8]. The fluorescence of silver nanocluster is easily observed when nucleolin of the live cell surface is connected with that templated by AS1411. These nanomaterials offer new approaches for bulk and single molecule biolabeling [9]. Aptamers can bind with a wide array of targets with high affinity and specificity. Based on the phenomenon, we can search aptamer which is related to tumor and applied biomedical system. In this work, G-quadruplex formed by G-rich oligonucleotide was selected as matrices to synthesize silver nanocluster. No paper about G-quadruplex templated silver nanocluster has been published so far.

In this paper, AS1411 is selected to investigate as typical G-quadruplex. AS1411 (also known as AGRO100) is based on a 26-base G-rich oligonucleotide which recently entered in phase II human clinical trials. AS1411 represents the first nucleic

* Corresponding author at: State Key Laboratory of Electroanalytical Chemistry, Changchun Institute of Applied Chemistry, Chinese Academy of Sciences, Changchun, Jilin 130022, People's Republic of China. Tel.: +86 431 85262003; fax: +86 431 85689711.
E-mail address: ekwang@ciac.jl.cn (E. Wang).

0039-9140/$ – see front matter © 2011 Elsevier B.V. All rights reserved.
doi:10.1016/j.talanta.2011.10.057

acid-based aptamer to be tested in patient for the treatment of cancer [10]. AS1411 is easily formed a dimeric G-quadruplex structure in the presence of K^+ and targeted nucleolin with high affinity and specificity. At the same time, AS1411 is multifunctional aptamers in bioanalysis and has been applied in the chemiluminescence (CL) detection of the protein marker nucleolin expressed at the surface of HeLa cells [11]. The G-quadruplexes have also been shown to have antiviral activity and AS1411 is a multifunctional anticancer aptamer with the ability to combine with two ligands simultaneously. For example, AS1411 is incorporated with nucleolin in cancer cell and hemin. Furthermore, AS1411 is also able to bind another ligand protoporphyrin IX (PPIX). Herein, we report a novel approach to DNA G-quadruplex-templated formation of fluorescent silver nanocluster and its application to bioimaging. We demonstrate the method of generating G-quadruplex-encapsulated silver nanoclusters in aqueous solution. The G-quadruplex-encapsulated silver nanocluster chiefly made of 2–4 silver atoms was demonstrated by matrix assisted laser desorption ionization/time of flight mass spectrum (MALDI TOF MS).

2. Materials and methods

2.1. Chemicals and materials

Silver nitrate ($AgNO_3$, (Sigma-Aldrich, 99.9999%)), sodium borohydride (AF granules, 10–40 mesh, 98%, Sigma-Aldrich), and all chemicals of analytical grade were used as received without further purification. 3-[4,5-dimethylthiazolyl-2]-2,5-diphenyltetrazolium bromide (MTT) were obtained from Sigma-Aldrich (USA). The oligodeoxynucleotide used synthesizing silver nanocluster synthesis for cell imaging was AS1411, an antiproliferative G-rich oligodeoxynucleotide (GRO) which sequence is 5′-d(GGTGGTGGTGGTTGTGG TGGTGGTGG)-3′. The other GROs also used in silver nanocluster synthesis were human telomeres, OXY, PW17, T30695, PS2M, 93del and their sequences were 5′-d (GGGTTAGGGTTAGGGTTAGGG)-3′, 5′-d(GGGGTTTTGGGGTTTTGGGGTTTTGGGG)-3′, 5′-d (GGGTAGGGCGGGTTGGG)-3′, 5′-d(GGGTGGGTGGGTGGGT)-3′, 5′-d(GTGGGTAGGGCGGGTTGG)-3′, 5′-d(GGGGTGGGAGGAGGGT)-3′, 5′-d(AATTCCCCCCCCCCCCCCCCAATT)-3′(called "C16″ for short) respectively. All the GROs were synthesized and HPLC purified by Shanghai Sangon Biotechnology Co. Ltd. (Shanghai, China). Before using, these GRO powders were dissolved in the 100 mM KCl, 20 mM potassium phosphate buffer (pH 7.4). The concentrations of them were quantified by using UV/vis/near IR spectrophotometer and determined using the 260 nm UV absorbance and the corresponding extinction coefficient: $A = 15{,}400$, $C = 7400$, $G = 11{,}500$, $T = 8700$. Phosphate Buffered Saline (PBS) [10 mM phosphate (NaH_2PO_4 and Na_2HPO_4), pH 7.4] was also prepared. The PBS buffer is used to rinsing suspension of HeLa cells. All the solutions were prepared by using distilled water and stored at 4 °C before use. HeLa cells were obtained from the American Type Culture Collection (Manassas, VA) and maintained in DMEM supplemented with 10% standard Fetal bovine serum (Defined FBS) (HyClone Laboratories, UT) at 37 °C and in 5% CO_2. Glass chamber slides (14 mm bottom well) were purchased from Hangzhou Sanyou Biotechnology Co. Ltd. (Hangzhou, China).

2.2. Apparatus

UV/vis absorption spectra were carried out by a CARY 500 UV/vis/near-IR spectrophotometer (Varian). Fluorescence measurements were recorded at room temperature using a LS 55 luminescence spectrometer (Perkin-Elmer). CD signal was performed by JASCO-820 Circular Dichroism spectrometer (Tokyo, Japan). The sample for cell imaging was obtained by fixing the bound cells using silver nanocluster on a 35 mm tissue culture dish (World Precision Instruments) and acquired the fluorescence images using LEICA TCS SP2 laser scanning confocal microscope (Germany) with a 100× oil immersion objective. TEM images were obtained with a FEI TECNAI G^2 transmission electron microscope (Netherlands) operating voltage of 120 kV.

2.3. Synthesis of GRO_m:Ag_n solutions

The purified GROs were dissolved in a buffer containing 100 mM KCl, 20 mM potassium phosphate buffer (pH 7.4) at a concentration of 10 mg/mL and allowed to dissolve over several hours. Samples were then equilibrated for 10 min at 90 °C in a water bath, followed by spontaneous cooling to room temperature overnight (annealed samples). The DNA was also subjected to rapid cooling by heating a 50 μM sample in the same buffer to 90 °C for 10 min. The DNA samples were then refrigerated until use.

The GROs and $AgNO_3$ solutions (concentration ratio = 1:6) were mixed and cooled to 0 °C with ice. After 15 min, the solutions were reduced with $NaBH_4$ (concentration ratio of $AgNO_3$:$NaBH_4$ = 1:1) and shaken intensively to form silver nanoclusters (GRO_m:Ag_n). In practically, concentration ratio of $AgNO_3$:GRO:$NaBH_4$ was 6:1:6. The $NaBH_4$ was dissolved in deionized water and added within 30 s. The solvents for all solutions were deionized water unless otherwise mentioned.

CD spectra were recorded using a 1 mm optical path length-quartz cell and an instrument scanning speed of 100 nm/min with a response time of 2 s at room temperature. CD spectra were obtained by taking the average of three times scans made from 210 to 340 nm. All DNA samples at a final concentration of 10 μm were dissolved in 50 mM PBS buffer (pH 7.4).

2.4. Bioimaging

HeLa cells incubated with AS1411 encapsulated silver nanocluster. HeLa cells were plated onto 35 mm glass chamber slides. Stock solutions of AS1411 encapsulated silver nanocluster dissolved in TE buffer were prepared at concentrations of 10 μM. Diluted solutions in complete growth medium were then freshly prepared and placed over the cells for 2–3 h. All cells were washed with PBS buffer (3×) at room temperature. After that, cells were scanned by LEICA TCS SP2 laser scanning confocal microscope.

2.5. MTT assay

In order to evaluate the silver nanocluster dose on cellular toxicity, the complex treated cells were illuminated for a serial concentration. After treatment, cells were incubated in fresh medium for 24 h. The culture medium was replaced by 100 μL fresh medium containing 0.5 mg/mL 3-[4,5-dimethylthiazol-2-yl]-2,5-diphenyl tetrazolium bromide assays reagent (MTT assay), and then incubated at 37 °C and 5% CO_2 for 4 h. Then, the MTT containing medium was added with 100 μL of acid/isopropanol solution, in which the concentration of HCl was 0.04 M to dissolve the MTT product, formazan. Viability of non-silver nanocluster-treated control cells was arbitrarily defined as 100%. Finally, the absorption at 490 nm of each well was measured by an EL808 ultramicroplate reader (Bio-TEK Instrument, Inc., Winooski, VT, USA). The relative cell viability was recorded and shown (Fig. 4).

3. Results and discussion

3.1. General consideration of the bioimaging design

In this paper, we demonstrate the method of generating G-quadruplex-templated silver nanoclusters in aqueous solution.

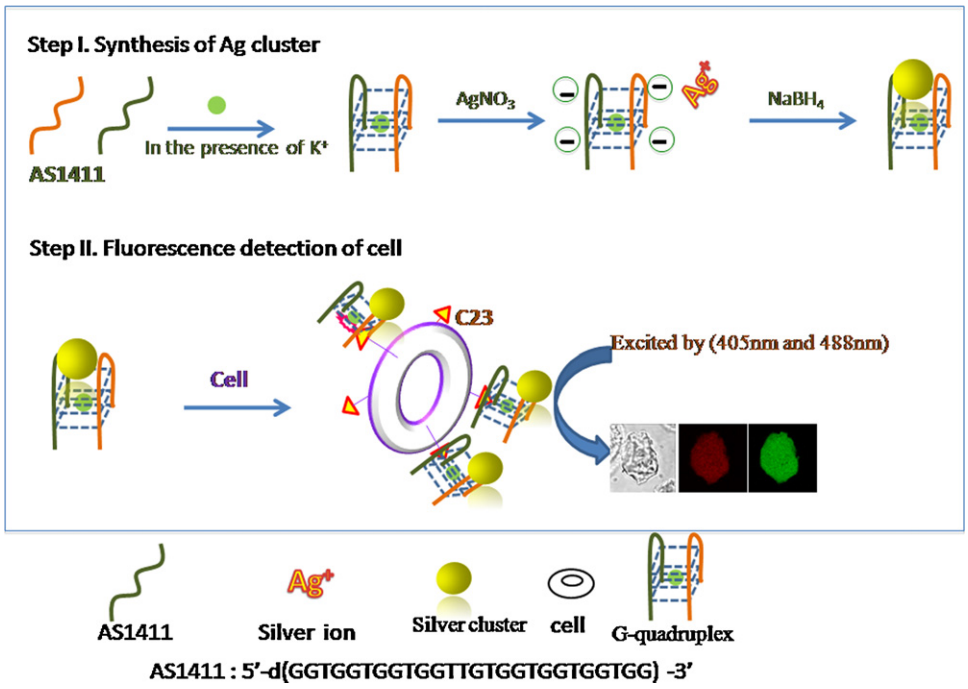

Scheme 1. Schematic diagram of fluorescence bioimaging based on silver nanocluster. Step 1. Guanine-rich oligonucleotide the formed G-quadruplex by the presence of K^+. Accordingly, silver nanocluster was produced by $NaBH_4$ reduction to complex of quadruplex and Ag^+. Step 2. Cell incubated with silver nanocluster was bioimaged by confocal spectroscopy.

Silver nanoclusters connected nucleolin in HeLa cells result in fluorescence signal enhancement. The spectrum of MALDI TOF MS indicated that 2–4 silver atoms attached to the G-quadruplex. This work successfully develops the capping G-quadruplex scaffolds of silver nanoclusters. So, in this paper, we applied AS1411 as matrices to generate silver nanocluster, then the silver nanocluster was processed for protein imaging in tumor cell. In order to detect universality of G-quadruplex templated silver nanoclusters, OXY, PW17, T30695, PS2M, 93del was investigated.

The experiment procedure of generating silver nanocluster and its application have been introduced (Scheme 1). Step I, small silver nanoclusters are synthesized by GROs as matrices. In the presence of K^+, GRO can form parallel G-quadruplex conformation. We report a novel method to get silver nanoclusters with G-quadruplex as a scaffold. The preparation of silver nanoclusters is very simple. Briefly, the G-quadruplex and silver nitrate were mixed and the silver ions were reduced by $NaBH_4$. At first, the oligonucleotide and $AgNO_3$ (Aldrich) are mixed. After 15 min, this mixture was reduced with $NaBH_4$. The total molar ratio of $AgNO_3$:oligonucleotide:$NaBH_4$ is 6:1:6. The experimental step in detail is shown in Section 2. The G-quadruplex is a good matrix to at least partially protect the silver nanoclusters from aggregation. Meanwhile, the silver nanocluster is water-soluble. Step II, HeLa cells incubated with AS1411-templated silver nanocluster is investigated by LEICA TCS SP2 laser scanning confocal microscope. The result of cell imaging demonstrated that silver nanocluster connected with nucleolin emitted different fluorescence signals by exciting at 405 nm and 488 nm in cells system.

3.2. Fluorescence detection and MS detection of silver nanocluster

The fluorescence detection is based on silver nanocluster. Fig. 1A depicts the fluorescence emission and excitation spectra of silver nanoclusters dissolved in water. From the figure, we can conclude that the intensity of excitation at 325 nm is strong while the ones of 510 nm (Fig. 1A) is relatively weak. The result of Fig. 1A indicated that the excitations at 325 nm resulted in an emission at 420 nm, while the excitations at 510, resulted in the emissions at 680 nm (Fig. 1A). As shown in Fig. 1B and C, we concluded that AS1411 encapsulated silver nanoclusters were made of 2 silver atoms (Ag_2). The fluorescence spectrum belong dimer (Ag_2) cluster.

3.3. CD assay and fluorescence quantum yields of silver nanocluster

To investigate the stability of parallel G-quadruplex conformation towards silver nanocluster, CD signal is recorded. The conformational change of AS1411 and AS1411 templated silver nanoclusters is confirmed by CD (Fig. 2). It has a positive band near 260 nm and a negative one at about 240 nm. From the CD spectrum, AS1411-encapsulated silver nanoclusters have a parallel G-quadruplex conformation. It demontrates that G-quadruplex conformation is not destroyed by transforming into silver nanocluster. The reason of selecting AS1411 is that the AS1411 aptamer forms a dimeric parallel G-quadruplex structure to combine nucleolin with high affinity and specificity. Significant function of AS1411 is its binding to the corresponding protein ligand (HIV-1 integrase or nucleolin), which gives its potential as anti-HIV or anticancer therapeutic agents [12]. The AS1411-encapsulated silver nanocluster specially connected with nucleolin of cell surface and then emitted fluorescence signal of silver nanocluster in cell system. According to reported previously [13], using 2-aminopyridine (0.1 M H_2SO_4) as a standard sample, the fluorescence quantum yields of silver nanocluster is 6.79%. We demonstrate the applicability of bright GRO-encapsulated silver clusters to bioimaging in a more specific way through cell surface nucleolin labeling.

3.4. Detection of a series of G-rich sequence-templated silver nanocluster

It has been proven that a great of functional nucleic acids, such as human telomere, and certain aptamers, are with G-rich

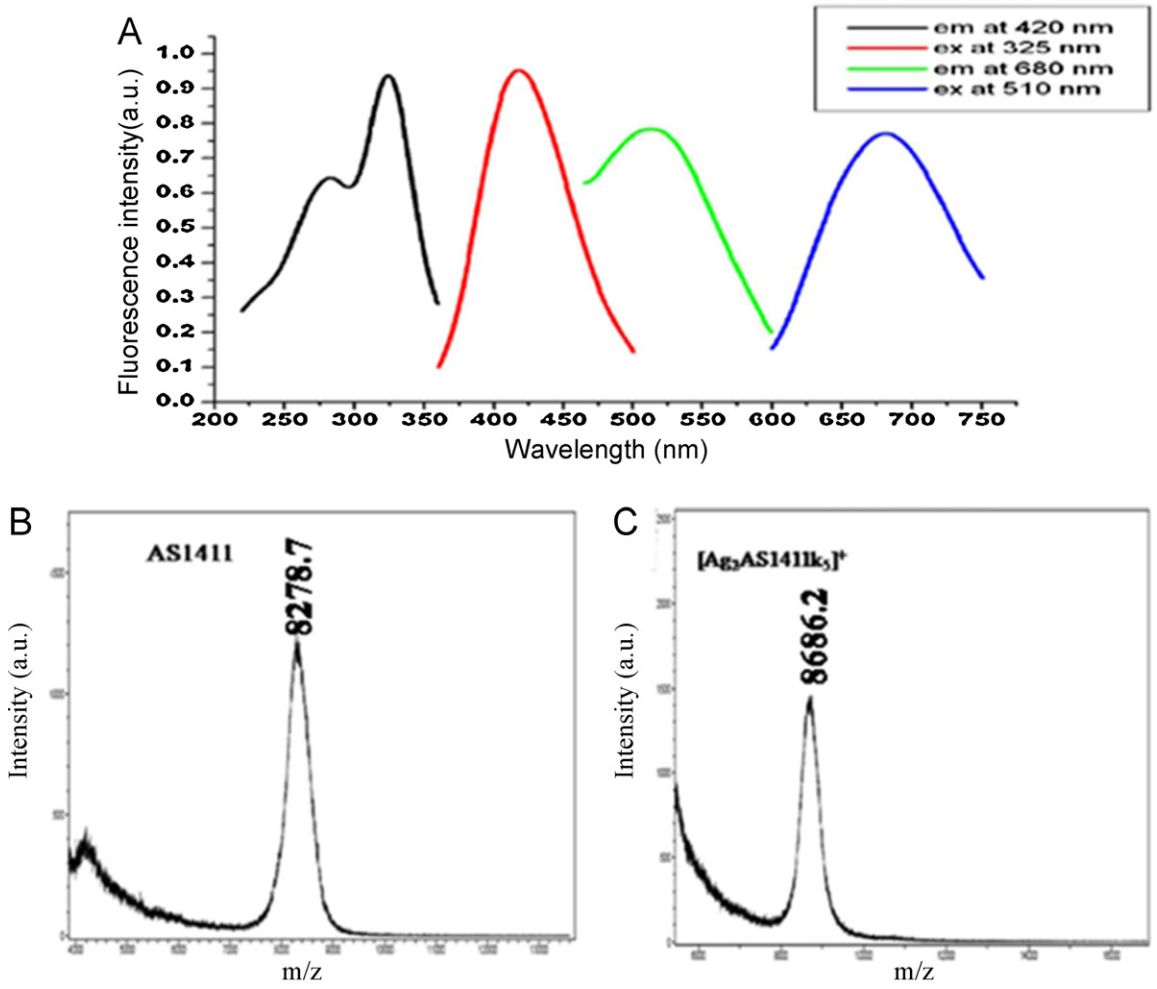

Fig. 1. (A) Fluorescence excitation/emission of AS1411 encapsulated silver nanocluster. (B) MALDI TOF MS spectrum of an aqueous solution AS1411. (C) MALDI TOF MS spectrum of an aqueous solution of $AgNO_3$/GRO/$NaBH_4$ picture of AS1411-encapsulated silver nanocluster (mole ratio of $AgNO_3$:GRO:$NaBH_4$ was 6:1:6, concentration of GRO = 10 μM).

sequences (GROs) and can fold into G-quartets under functioning condition. Here we picked up several such sequences to demonstrate that the method to synthesize silver nanocluster is general, and with a promising potential to be used into more applications. These GROs are respectively 93del, human telomeres, OXY, PW17, T30695, PS2M. The silver nanocluster synthesized based on them has been monitored by fluorescence microscopy and MALDI TOF MS, as shown in Fig. 1B, and Figs. S7–S11. From the experiment

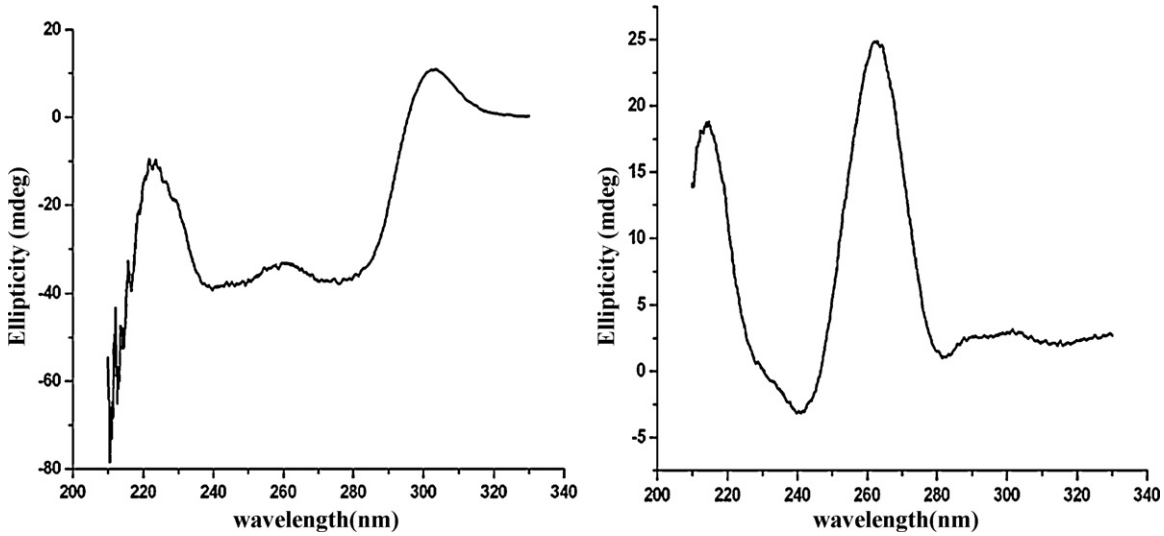

Fig. 2. The left side is the CD spectrum of AS1411 G quadruplexes in PBS buffer stabilized by 100 mM K^+; the right side is the CD spectrum of AS1411-encapsulated silver nanoclusters (mole ratio of $AgNO_3$:AS1411:$NaBH_4$ was 6:1:6, concentration of AS1411 = 10 μM) in PBS buffer (pH 7.4, 100 mM K^+).

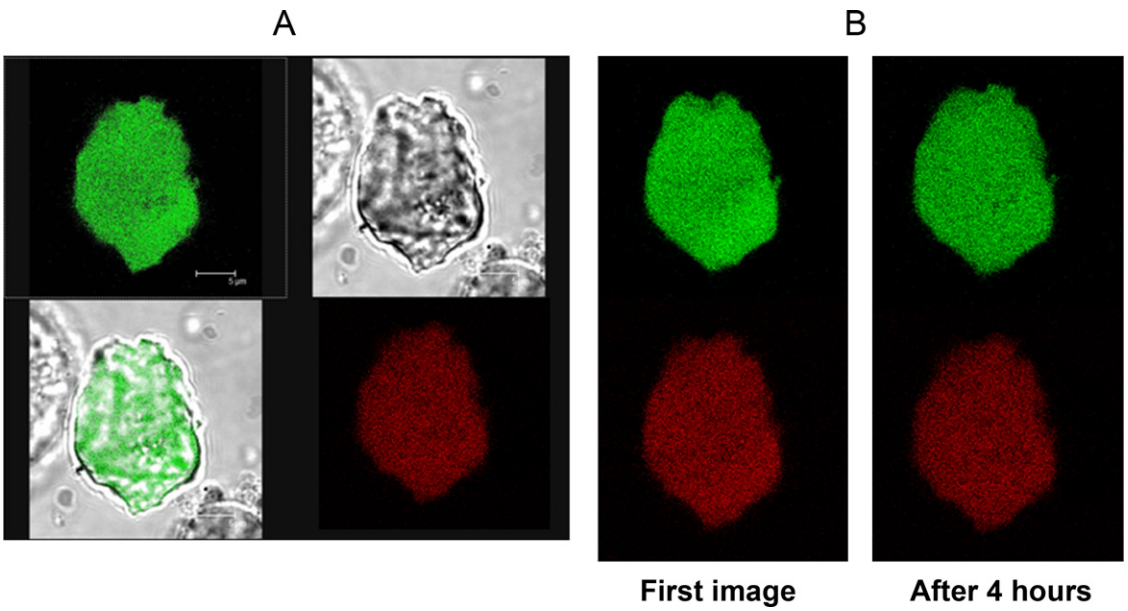

Fig. 3. Fluorescence image of HeLa cell incubated with silver nanocluster on glass chamber slides. Confocal spectroscopy scanning image obtained on collecting fluorescence of silver nanocluster enfolded byAS1411-C23 upon excitation at 405 nm and 488 nm (A); 100× oil immersion and sequence scan with time was at 37 °C and 5% CO_2; (B) an image sequence is recorded of 48 images at regular time intervals of 5 min. The first image shows after 30 min imaging picture that the HeLa cells incubated with silver nanoclusters. The fluorescence signal after 30 min and after 4 h had a little difference.

result, we know that 93del, OXY, PW17, T30695 encapsulated silver nanoclusters are made of 2 silver atoms (Ag_2). However, PS2M encapsulated silver nanoclusters are made of 3 silver atoms (Ag_3) and human telomeres encapsulated silver a made of one silver atom (Ag_1). The fluorescence spectrum of above silver clusters are illustrated by Figs. S6–S10.

3.5. *Bioimaging, MTT assay and TEM detection of the size of silver nanocluster, (Fig. 5)*

The spectra of CD spectroscopy shows that AS1411-encapsulated silver nanoclusters have a strong G-quadruplexes signal (illustrated in Fig. 2). It is proved that AS1411 might be connected with nucleolin in cancer cell surface. So, HeLa cell incubated with AS1411-encapsulated silver nanocluster. Using confocal fluorescence microscopy, the bioimaging of adding silver nanocluster to the HeLa cells was investigated. Fig. 3 shows confocal fluorescence images of HeLa cells incubated with 5 μM of the silver nanocluster complexes. It is demonstrated that AS1411: Ag_n is brighter and more photostable than dyes. A lot of dyes are easily photobleached in cells [10,14]. The green and red fluorescence of silver nanocluster in HeLa cells is anti-photobleaching. After 4 h, the diversification of fluorescence intensity is very small (shown in Fig. 3B). Fig. 3A shows that silver nanocluster incorporated with nucleolin is excited at 405 nm and 488 nm in cell system. From the result, silver nanocluster can emit different wavelength light, this is different from other kinds of cell imaging [15]. Fig. 3B shows that the image is recorded by intervals of 5 min. The first image is the fluorescence imaging of the HeLa cells incubated with silver nanoclusters over 30 min. The fluorescence signal after 30 min and after 4 h shows nearly no difference. In general, the fluorescence signal is quenched by mercapto group in cell. The photoluminescence mechanism is not clear to date.

The cytotoxicity of the silver nanocluster on the cell proliferation used in our system was investigated by MTT assay. Fig. 4 showed the data of cell viability of the HeLa cells after 24 h of incubation with the transfection complexes. Non-transfected cells were severed as

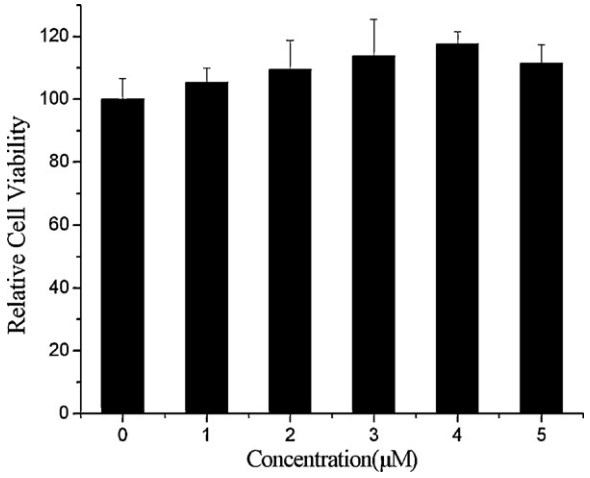

Fig. 4. Cytotoxicity of the silver nanocluster on HeLa cells was measured by MTT assays ($n = 8$, mean ± S.D.). The result showed the relative cell viability of the cells accompany with silver nanocluster with the final concentrations of 0, 5, 8, 10, 15 and 20 μM. The viability of positive control that treated with same volume of water was taken as 100%.

the control and the cell viability of which were set as 100%. It was found that the silver nanocluster for the transfection had hardly any toxicity to the cells. In the presence of silver nanocluster, the cell viabilities increased to be more than 80% for both of the transfection systems. With addition of silver nanocluster at the concentration of 20 μM, the cell viabilities for silver nanocluster did not decrease.

To consummate this assay system, a control experiment was carried out. Herein, C-rich oligonucleotide C16 is selected to control aptamer. It is well known that the size of the nanoclusters is related to its characteristic. So, we detect the size of AS1411 and C16 templates silver nanocluster. TEM analysis (Fig. 5A) established that 97% of the water-soluble AS1411-encapsulated silver nanoclusters ranged between 1.0 and 2.8 nm in diameter with a distribution peak at 1.7 nm. However, the size of C16-encapsulated

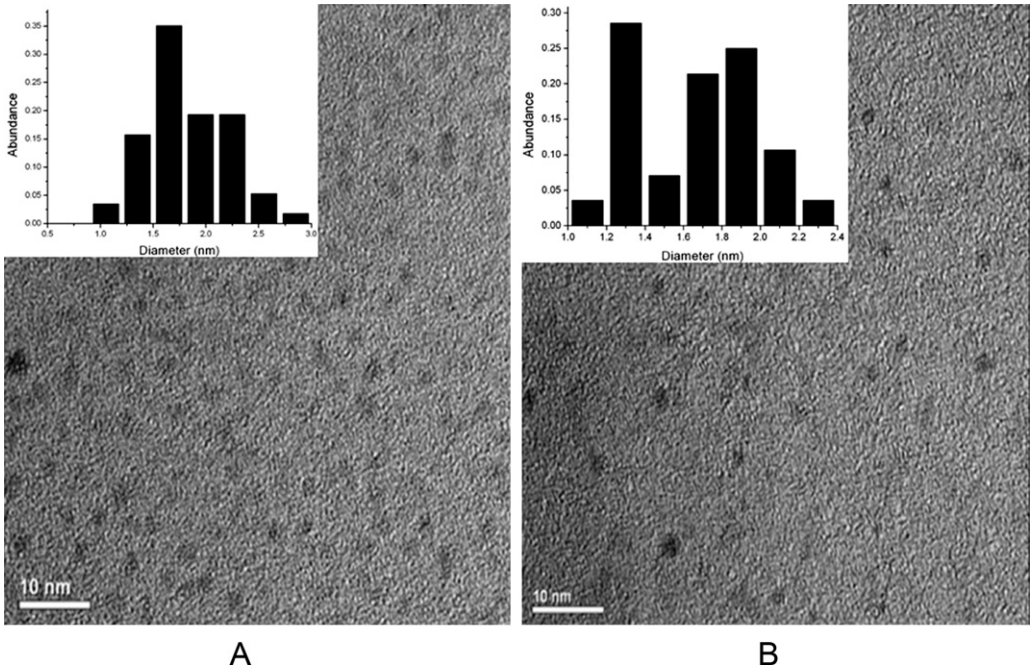

Fig. 5. TEM images of (a) AS1411 templated silver nanoclusters (A) and (b) AATTCCCCCCCCCCCCCCCCAATT templated silver nanoclusters (B). Inset: corresponding histograms of the core diameters of (a) A and (b) B.

silver nanoclusters is 1.8–2.5 nm (Fig. 5B). TEM images of G-quadruplex templated silver nanocluster solutions show entities with sizes smaller than 2 nm in diameter. In the solution, the clusters are still protected by the G-quadruplex, thereby they are stable over prolonged periods, and they do not aggregate to form large nanoparticles [16]. Such a characterization of TEM is often applied to the analysis of silver cluster [16–19]. MALDI-TOF mass spectrum of the clusters shows the presence of clusters containing a small number of Ag atoms, such as Ag_2, Ag_3, and some Ag_4 [16]. It is well known that the optical properties of metals depend largely on their size, especially in the nanometre range.

4. Conclusions

In summary, we demonstrate the novel method of generating G-quadruplex-encapsulated silver nanoclusters in aqueous solution. In these G-quadruplexes, the fluorescence quantum yields of AS1411-encapsulated silver nanocluster is 6.79%. Although fluorescence signal of the AS1411-encapsulated silver nanocluster in aqueous solution is weak, however, the signal of silver nanocluster incubated with cells is very strong. It is found that the formation of silver nanoclusters is highly fluorescence signal enhancement action by AS1411 specially connected nucleolin in HeLa cells. The data of MALDI TOF MS verified that small numbers of silver atoms are bound to the oligonucleotide G-quadruplex. This work develops successfully the capping G-quadruplex scaffolds of silver nanoclusters, and the high photobleaching may have great potential in early detection of cancer and bioanalysis field. A mechanism of generating fluorescence signal is accordingly proposed. These new insights into the G-quadruplex-encapsulated silver nanoclusters will help us to further extend their applications in the bioanalytical field, especially single-molecule studies faster and in longer time scales.

Acknowledgement

This work was supported by the National Natural Science Foundation of China, grant nos. 21075120, 20935003, and 973 projects 2009CB930100, 2010CB933600.

Appendix A. Supplementary data

Supplementary data associated with this article can be found, in the online version, at doi:10.1016/j.talanta.2011.10.057.

References

[1] T. Vosch, Y. Antoku, J.C. Hsiang, C.I. Richards, J.I. Gonzalez, R.M. Dickson, PNAS 104 (2007) 12616–12621.
[2] J.P. Wilcoxon, B.L. Abrams, Chem. Soc. Rev. 35 (2006) 1162–1194.
[3] J. Zheng, P.R. Nicovich, R.M. Dickson, Annu. Rev. Phys. Chem. 58 (2007) 409–431.
[4] S. Link, S. FitzGerald, M.A. El-Sayed, T.G. Schaaff, R.L. Whetten, J. Phys. Chem. B 106 (2002) 3410–3415.
[5] J.T. Petty, J. Zheng, N.V. Hud, R.M. Dickson, J. Am. Chem. Soc. 126 (2004) 5207–5212.
[6] C.M. Ritchie, K.R. Johnsen, J.R. Kiser, Y. Antoku, R.M. Dickson, J.T. Petty, J. Phys. Chem. C 111 (2007) 175–181.
[7] K. Koszinowski, K. Ballweg, Chem. Eur. J. 16 (2010) 3285–3290.
[8] H.C. Yeh, J. Sharma, J.J. Han, J.S. Martinez, J.H. Werner, Nano Lett. 10 (2010) 3106–3110.
[9] J. Yu, S. Choi, C.I. Richards, Y. Antoku, R.M. Dickson, Photochem. Photobiol. 84 (2008) 1435–1439.
[10] C.R. Ireson, L.R. Kelland, Mol. Cancer Ther. 5 (2006) 2957–2962.
[11] T. Li, L. Shi, E. Wang, S. Dong, Chem. Eur. J. 15 (2009) 1036–1042.
[12] K. Braeckmans, L. Peeters, N.N. Sanders, S.C. De Smedt, J. Demeester, Biophys. J. 85 (2003) 2240–2252.
[13] R. Rusakowi, A.C. Testa, J. Phys. Chem. 72 (1968) 2680–2681.
[14] S.H. Chou, K.H. Chin, A.H.J. Wang, Trends Biochem. Sci. 30 (2005) 231–234.
[15] M.H. Ko, S. Kim, W.J. Kang, J.H. Lee, H. Kang, S.H. Moon, D.W. Hwang, H.Y. Ko, D.S. Lee, Small (2009) 1207–1212.
[16] I. Dĩez, M. Pusa, S. Kulmala, H. Jiang, A. Walther, A.S. Goldmann, A.H.E. Müller, O. Ikkala, R.H.A. Ras, Angew. Chem. Int. Ed. (2009) 2122–2125.
[17] B. Adhikari, A. Banerjee, Chem. Mater. (2010) 4364–4371.
[18] S. Roy, A. Banerjee, Soft. Matter (2011) 5300–5308.
[19] Y.C. Chung, I.-H. Chen, C.-J. Chen, Biomaterials (2008) 1807–1816.